Scientific Research

Influence of H-Type and L-Type Activated Carbon in the Photodegradation of Methylene Blue and Phenol under UV and Visible Light Irradiated TiO$_2$

Juan Matos[*], Karina Quintana, Andreina García

Engineering of Materials and Nanotechnology Centre, Venezuelan Institute for Scientific
Research (I.V.I.C.), Caracas, Venezuela
Email: [*]jmatoslale@ivic.gob.ve

ABSTRACT

Photodegradation of methylene blue (MB) and phenol (Ph) on TiO$_2$ in presence of H-type and L-type activated carbons (AC) was studied. Photodegradation of MB and Ph were studied under two different lamps and results were compared against those obtained on a commercial TiO$_2$. Apparent first order rate constant for the degradation of MB was higher in presence of any AC in comparison of TiO$_2$ alone while only in presence of AC$_{CO2-800}$ phenol was photodegradated in shorter irradiation time than that required by TiO$_2$. It can be concluded that TiO$_2$ enhances its photoactivity by a factor up to 8.7 in the degradation of MB in presence of AC and this effect is associated to the specific surface properties of AC.

Keywords: Photocatalysis; TiO$_2$; Activated Carbon; Methylene Blue; Phenol

1. Introduction

An important quantity of the total world production of azo-dyes is released in textile effluents [1]. Different technologies for the removal of dyes are adsorption, bio- and chemical degradation methods including advanced oxidation technologies as heterogeneous photocatalysis. Since heterogeneous photocatalysis with TiO$_2$ emerged as an efficient method for purifying water and air [2,3] several attends such as ion doping or metal depositions have been used [4] to increase its photoefficiency. Another way to possibly increase the photoefficiency of TiO$_2$ consists of adding an inert co-adsorbent such as activated carbon (AC) [5,6]. A synergy effect between both solids has been observed in the photocatalytic degradation of model pollutants [7,8]. This has been ascribed to a contact interface that promotes an appropriated diffusion of pollutants from AC to photoactive titania and introduce changes in the semiconductor properties [5-8]. Photocatalysis and adsorption with activated carbon (AC) have received an increase attention for the degradation of different dyes [9-11] and halo phenol molecules [7] where recently, we have showed that surface functionalization of AC play an important role on TiO$_2$ photoactivity on 4-chlorophenol degradations [7]. The objective of this work is to study the photodegradation of methyl-ene blue (MB) as a model dye and phenol (Ph) as a model aromatic molecule on UV- and visible light irradiated TiO$_2$ in presence of H-type and L-type AC which are characterized by different texture and surface functionalities.

2. Experimental

Methylene blue (MB) and phenol (Ph) were analytical grade and purchased from Aldrich. For comparative purpose, photocatalyst was TiO$_2$ P25 (Degussa). H-type AC were prepared by physical activation of a soft wood under CO$_2$ flow at 800˚C (AC$_{CO_2\text{-}800}$) or by pyrolysis under N$_2$ flow at 1000˚C (AC$_{N_2\text{-}1000}$) while L-type AC were prepared by impregnation with 5% (w/w) of ZnCl$_2$ (AC$_{ZnCl_2\text{-}5\%}$) and H$_3$PO$_4$ (AC$_{H_3PO_4\text{-}5\%}$) following activation under N$_2$ flow at 450˚C. Samples were characterized by adsorption-desorption N$_2$ isotherms, infrared spectroscopy (FTIR) and surface pH (pH$_{PZC}$). The experimental set-up [11] consists in an open to air batch photoreactor of 200 mL made of Pyrex. Irradiation was provided with two different lamps [11] with different UV proportions. One a Hg lamp (82.9 W·m^{-2} of UV and 362.6 W·m^{-2} for visible light) and metal halide (MH) lamp (70.2 W·m^{-2} of UV and 452.5 W·m^{-2} of visible) and a last one, a sodium (Na) lamp, 99% visible light (8.4 W·m^{-2} of UV and 831.6 W·m^{-2} for visible light). Photocatalytic tests were per-

formed at 25˚C with 62.5 mg TiO$_2$ and 6.2 mg AC under stirring in 125 mL of MB, 25 ppm (78.2 μmol·L^{-1}) initial concentration or in 125 mL of phenol, 50 ppm (0.5 × 10^{-3} mol·L^{-1}) initial concentration. Samples were maintained in the dark by 60 min to complete adsorption at equilibrium before irradiation. After centrifugation of MB aliquots at some selected reaction times, samples were analyzed by UV-spectrophotometer at 664 nm. For the case of phenol and their main intermediate products, hydroquinone (HQ) and benzoquinone (BQ), Millipore disks (0.45 μm) were used to remove particulate matter before HPLC analysis. Although non-agglomerate solid particles may pass through these membranes, our experience showed that the performance of the chromatographic column was not impaired for a long period of use. The HPLC system adjusted at 270 nm for the detection of phenol and of the main intermediate products was used. A reverse-phase column with a mobile phase composed of acetonitrile and deionized doubly distilled water was used. The v/v ratio CH$_3$CN/H$_2$O was 10/90 and the flow rate was 1 ml/min.

3. Results and Discussion

3.1. Characterization

Table 1 shows textural properties and pH$_{PZC}$ of photocatalysts. AC developed high surface areas BET (S$_{BET}$) and the main pore width in the the microporous range. For the case of mixed system TiO$_2$-AC, S$_{BET}$ decreases one order magnitude with respect to activated carbon.

Table 1. BET surface area (S$_{BET}$), mean pore diameter (D) and surface pH (pH$_{PZC}$).

Sample	S$_{BET}$ (m^2·g^{-1})	D(Å)	pH$_{PZC}$
TiO$_2$ P25	45.17 ± 0.16	577.86	6.5
AC$_{CO_2-800}$	942.86 ± 1.41	6.29	8.5
TiO$_2$– AC$_{CO_2-800}$	86.46 ± 0.48	974.01	6.7
AC$_{N_2-1000}$	644.27 ± 0.62	5.90	8.9
TiO$_2$– AC$_{N_2-1000}$	60.40 ± 0.39	1051.78	6.7
AC$_{ZnCl_2-5\%}$	689.39 ± 0.61	5.89	6.0
TiO$_2$– AC$_{ZnCl_2-5\%}$	92.51 ± 0.50	979.03	6.4
AC$_{H_3PO_4-5\%}$	246.66 ± 0.44	5.94	4.0
TiO$_{2-}$$_{H_3PO_4-5\%}$	63.38 ± 0.39	1034.43	6.3

This fact can be attributed to a strong interaction between both solids [12]. It can be seen from **Table 1** that H-type AC presented basic pH$_{PZC}$ while L-type AC showed acid pH$_{PZC}$ which suggest the presence of basic and acid oxygenated functional groups on the surface of H- and L-type AC, respectively. This inference can be verified by FTIR analysis which is shown in **Figure 1**. It can be seen that functional surface groups principally are basic as cyclic ethers (-C-O-C-) and quinones (C=O) [7,13]. For the case L-type AC, these showed acid pH$_{PZC}$ and by FTIR can be observed that the main functional surface group was carboxylic acid (C=O). Furthermore, cyclic ethers were also detected (-C-O-C-). Finally, it should
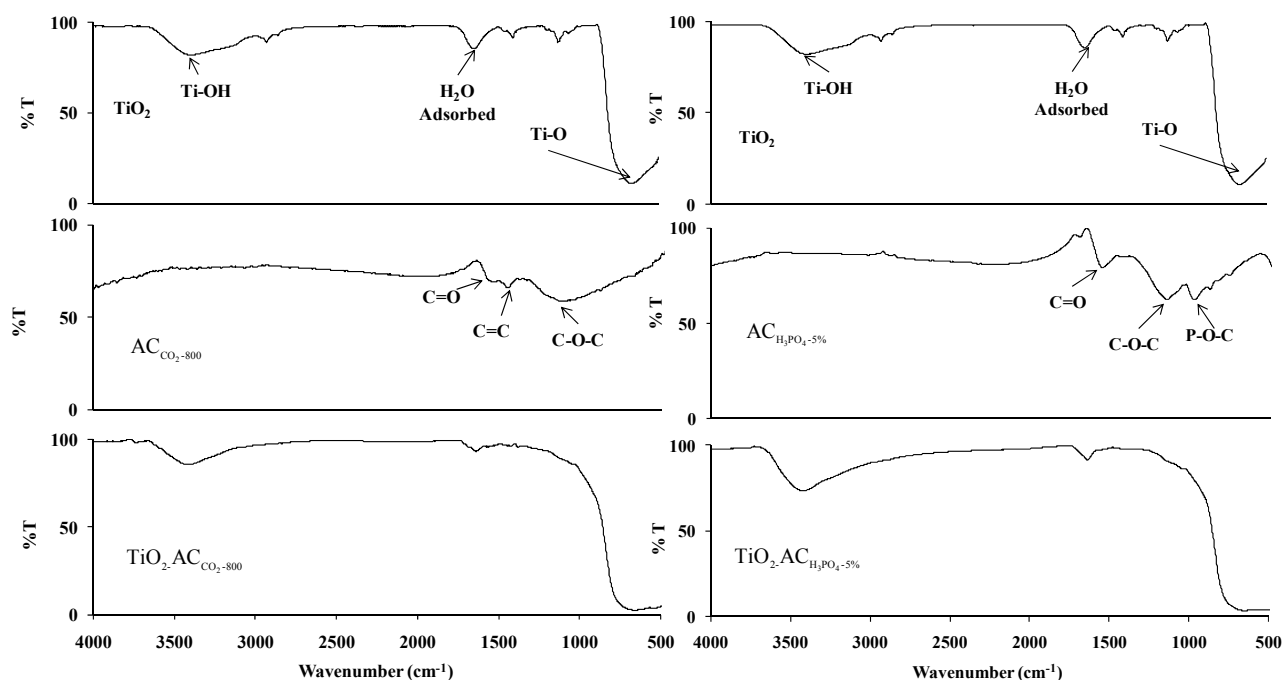

Figure 1. FTIR spectra of TiO$_2$, AC$_{CO_2-800}$, AC$_{H_3PO_4-5\%}$, TiO$_{2-}$AC$_{CO_2-800}$, and TiO$_{2-}$AC$_{H_3PO_4-5\%}$.

be remarked the presence of phosphates in $AC_{H_3PO_4}$ [7,8]. **Figure 1** shows that TiO_2 presented a broader peak in the region of bulk Titania in presence of AC. Also, the corresponding peaks in the AC clearly decreased in the binary materials probably by the coordination from carbon to the metallic centre in TiO_2 [7]. A similar behavior in the FTIR spectra for the other AC and the binary materials was found [7]. **Figure 2** shows the XRD patterns of TiO_2, AC and the binary materials TiO_2-AC. It can be seen that no changes in the corresponding XRD patterns

for the case of TiO_2-AC in comparison than that obtained for TiO_2 alone. The only change detected in the XRD pattern of the binary materials was a remarkable decrease in the main peaks attributed to a dilution effect by means of the presence of AC.

3.2. Adsorption in the Dark of MB and Photodegradation

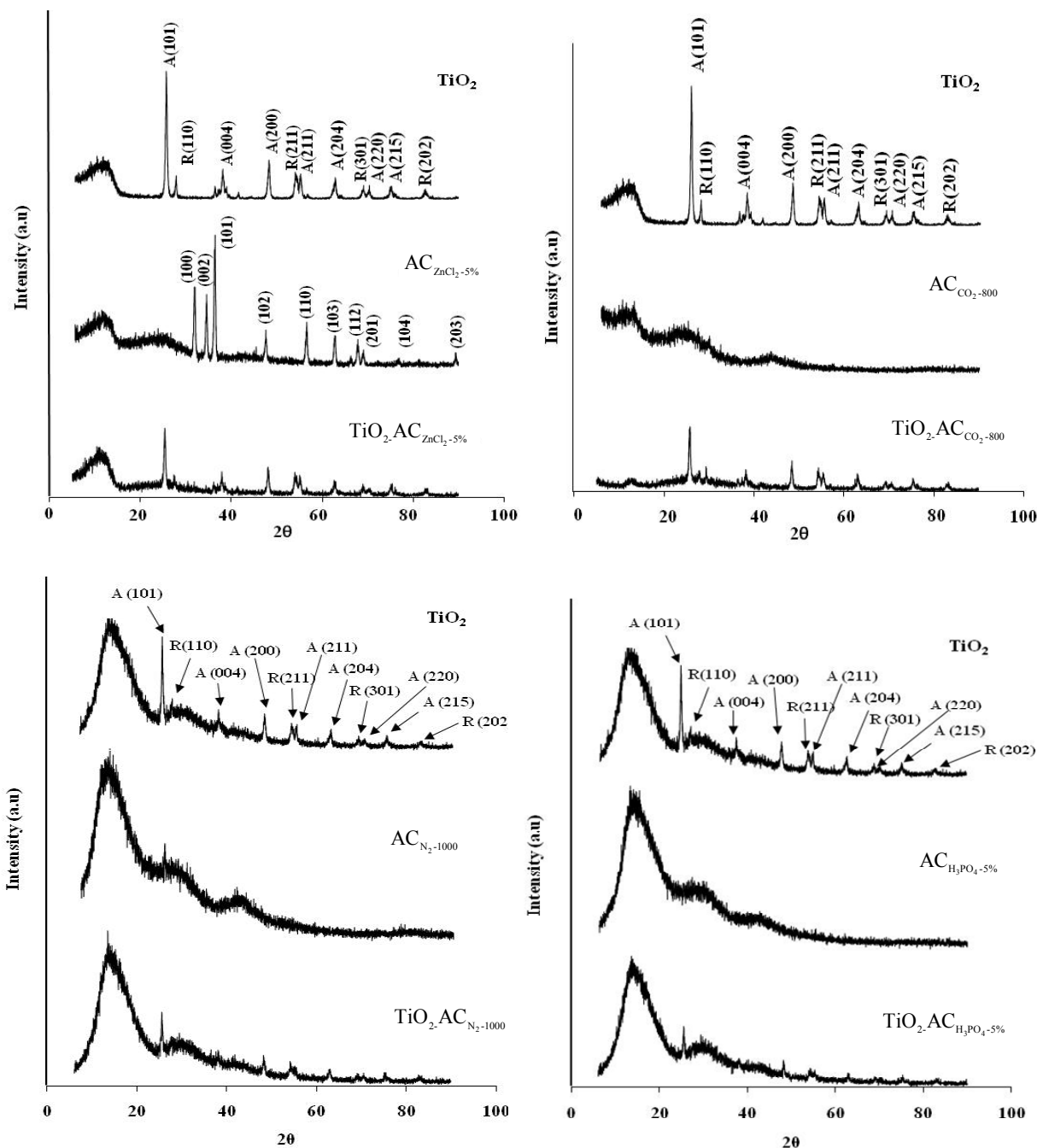**Figure 3** shows the kinetics of adsorption in the dark of

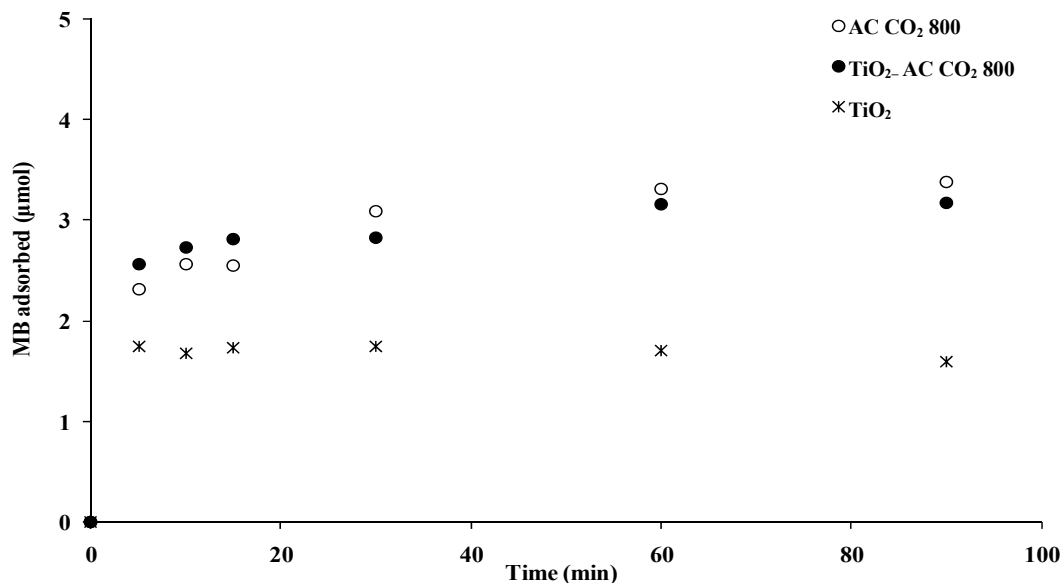Figure 2. XRD patterns of TiO_2, AC and binary materials TiO_2-AC.

Figure 3. Micromoles adsorbed in presence of some selected solids.

MB on AC and TiO$_2$-AC. In all cases, adsorption occurred within 30 min but to ensure the equilibrium of adsorption, a period of 60 min of adsorption in the dark was selected prior to the photodegradation experiments. The results indicated that there are no additive effects in the adsorption capacities of both solids after they are mixed. It can be ascribed to a strong interaction between TiO$_2$ particles and AC [7]. Kinetics of photocatalytic disappearance of MB in presence of TiO$_2$-AC under each lamp was performed. **Figure 4** shows an example of the kinetic of MB photodegradation under UV irradiated TiO$_2$, TiO$_2$- AC$_{CO_2-800}$, and TiO$_2$- AC$_{N_2-1000}$ samples. Assuming a first-order reaction rate [7], linear transformations (figure inset **Figure 4**) from the kinetic data were performed to estimate the apparent first-order rate constant (k$_{app}$). **Table 2** contains a summary of the kinetic results obtained for the MB photodegradation. The apparent first-order rate constant permits to estimated the photoactivity relative to TiO$_2$ defined as

$\varphi_{rel} = \left[k_{app-i}/k_{app-TiO_2} \right]$ and the synergistic effect in the photoactivity between TiO$_2$ and AC materials defined by the expression: $I_F = \left[k_{app-i}/k_{app-TiO_2} + k_{app-AC} \right]$.

It can be seen from k$_{app}$ values in **Table 2** that for both lamps used the binary materials TiO$_2$-AC have higher photoactivity than that obtained on TiO$_2$ alone and this enhancement in the photoactivity was clearly higher with the MH lamp which has higher proportion of visible light with respect to the Hg lamp with an enhancement in the photoactivity up to 8.7 and 6.0 times higher than TiO$_2$ on TiO$_2$- AC$_{CO_2-800}$ and TiO$_2$- AC$_{N_2-1000}$. Both AC$_{CO_2-800}$ and AC$_{N_2-1000}$ can be classified as H-type [5] AC because its surface oxygenated functional groups are basic in nature as suggest the FTIR spectra from **Figure 1** and

the basic pH$_{PZC}$ in **Table 1**. In addition, it should be pointed out that the photocatalytic activity of activated carbons is lower than that of TiO$_2$ alone, however, a clear synergistic effect between both solids was estimated (**Table 2**) being clearly higher under visible light irradiation.

On the other hand, **Table 2** shows that photoactivity of the binary materials TiO$_2$-AC$_{ZnCl_2-5\%}$ and TiO$_2$-AC$_{H_3PO_4-5\%}$ were only about 3 times higher than that on TiO$_2$ alone in any of cases of lamps studied. This fact has been attributed to a more acidic surface pH and to a lower surface area of these L-type AC (**Table 2**) [6,8]. In previous works [5,7] we have showed that oxygenated functional groups in the surface of AC play a double role in photocatalytic reactions. First, these AC can play the role of electron carriers that could inhibit the recombination of photoelectrons to improve the photoactivity of TiO$_2$ and secondly, under visible light irradiation several functional groups on carbon's surface are able to excited electrons from π to π^* orbital to then be injected into the conduction band of TiO$_2$ [11]. This phenomena has been described by our group as a photo-assisting process [12,14].

3.3. Adsorption in the Dark of Phenol and Photodegradation

Kinetics of adsorption in the dark of phenol on AC and TiO$_2$-AC was performed before irradiation tests. **Figure 5** shows that phenol adsorption occurred within 30 min but 60 min of adsorption in the dark was selected prior to the photodegradation experiments to ensure the equilibrium of adsorption. The results indicated that there are no additive effects in the adsorption capacities of both solids after they were mixed indicating a strong interaction
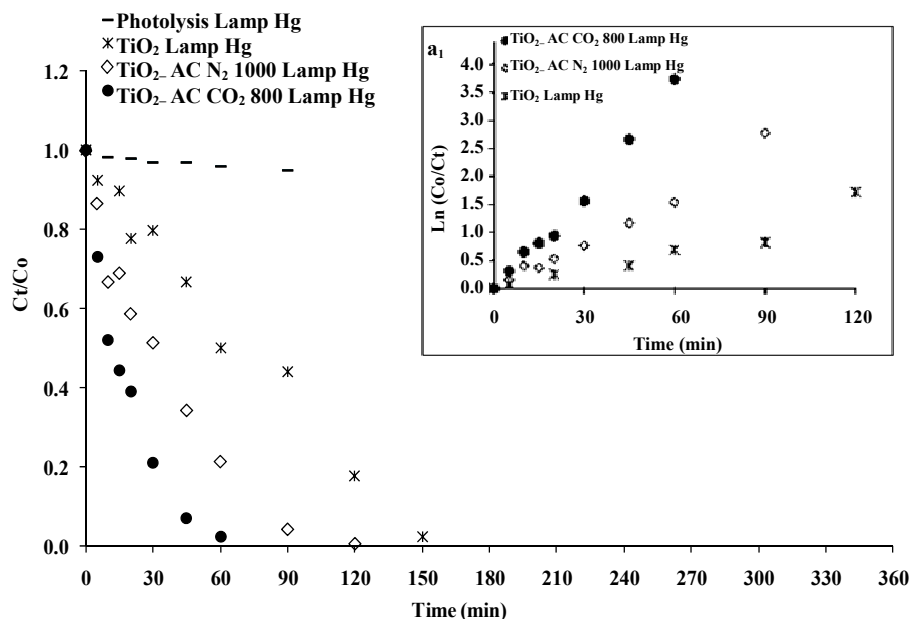
Figure 4. Kinetic of disappearance of MB on TiO₂-AC under Hg Lamp (A1) and lineal regression of kinetic data (a₁).

Table 2. Summary of kinetics parameters obtained in the photodegradation of MB.

Sample	Ads[a](%)	$k_{app-UV} \times 10^{-3}$ (min⁻¹)	I_{F-UV}[b]	φ_{rel-UV}[c]	$k_{app-Vis} \times 10^{-3}$ (min⁻¹)	I_{F-Vis}[b]	$\varphi_{rel-Vis}$[c]
TiO₂ P25	25	12.10	1.0	1.0	4.60	1.0	1.0
AC$_{CO_2-800}$	33	4.04	-	0.3	2.59	-	0.6
TiO₂– AC$_{CO_2-800}$	31	59.12	3.7	4.9	39.89	5.5	8.7
AC$_{N_2-1000}$	23	3.33	-	0.3	2.24	-	0.5
TiO₂– AC$_{N_2-1000}$	28	34.48	2.2	2.8	27.80	4.1	6.0
AC$_{ZnCl_2-5\%}$	27	1.10	-	0.1	2.54	-	0.6
TiO₂– AC$_{ZnCl_2-5\%}$	26	28.85	2.2	2.4	14.63	2.0	3.2
AC$_{H_3PO_4-5\%}$	14	0.71	-	0.1	1.01	-	0.2
TiO$_{2-H_3PO_4-5\%}$	23	39.41	3.1	3.3	13.39	2.4	2.9

[a]After 60 min of adsorption in the dark. [b]Synergy defined as $I_F = \left(k_{app-i} / k_{app-TiO_2} k_{app-AC} \right)$. [c]Relative photoact ivity defined as $\varphi_{rel} = \left(k_{app-i} / k_{app-TiO_2} \right)$.

between TiO₂ and AC [6,7].

Figure 6(a) shows the kinetics of disappearance of phenol in absence of solids (direct photolysis) and under some selected solids irradiated with UV light (Hg lamp). Linear transformations from the kinetic data were performed assuming a first-order reaction rate (**Figure 6(b)**). Apparent rate constant of first-order (k_{app}) and photocatalytic activity relative to TiO₂ alone (A_{photo}) defined as $k_{app-i} / k_{app-TiO_2}$, were estimated. These values are compiled in **Table 3**. It can be seen in **Figure 6** that disappearance of phenol by direct photolysis without solids and under irradiated AC were negligible. **Table 3** shows that k_{app} was higher under the Hg Lamp with respect to MH Lamp, for all systems studied. TiO₂- AC$_{CO_2-800}$ presented higher photoactivity that TiO₂ alone. The other binary materials

TiO₂-AC showed moderate photoactivity under Hg lamp and inhibition of the photoactivity under MH lamp. The enhancement in the photoactivity of TiO₂ can be due to the presence of a common contact interface between both solids as reported elsewhere for the case of 4-chlorophenol [7,8].

In spite of phenol adsorbed in the dark (**Table 3**) on TiO₂- AC$_{N_2}$ is lightly higher than that adsorbed on TiO₂- AC$_{CO_2}$, it can be seen from **Figure 6(a)** that photocatalytic activity of the TiO₂- AC$_{CO_2}$ binary material is higher than that of TiO₂- AC$_{N_2}$. This behavior can be attributed to two main reasons. First, TiO₂- AC$_{N_2}$ has a lower BET surface area than that of TiO₂- AC$_{CO_2}$ (**Table 1**) with a concomitant less capability to adsorb both phenol as the main intermediate products. In addition,
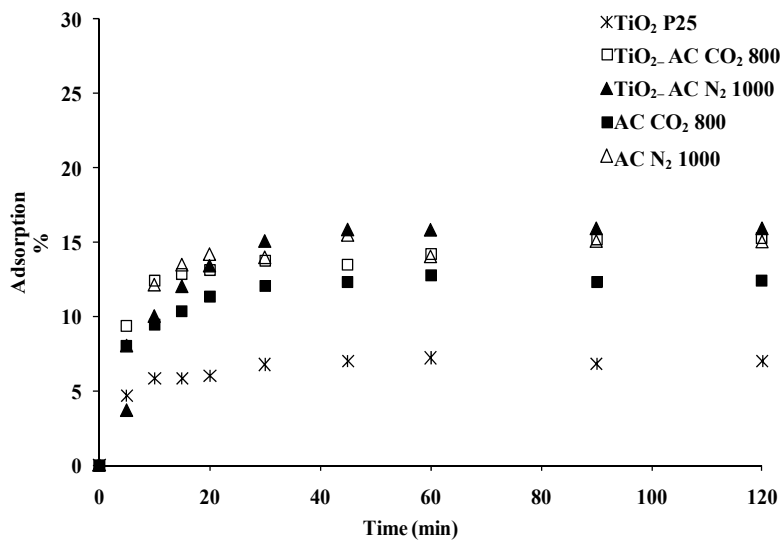
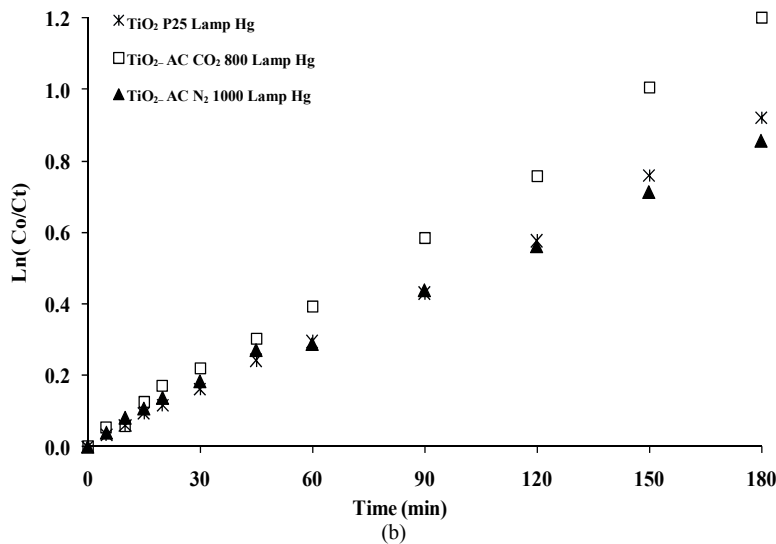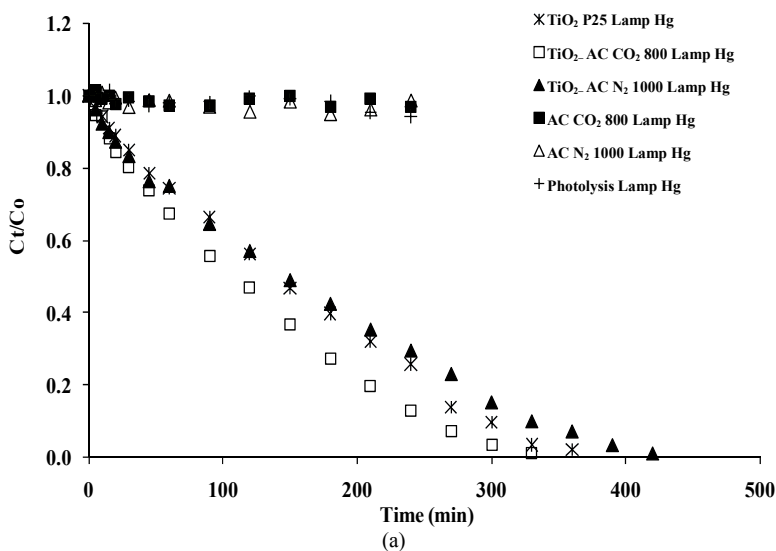**Figure 5. Phenol adsorbed in the dark on some selected solids.**

(a)

(b)

Figure 6. (a) Kinetic of disappearance of phenol on TiO₂–AC under Hg Lamp; (b) Lineal regression of the kinetic data.

Table 3. Kinetic parameters in the degradation of phenol.

Sample	Ads %	UV irradiation (Hg lamp)			Visible irradiation (MH lamp)		
		$k_{app} \times 10^{-3}$ (min^{-1})	$R^{2\,a}$	$A_{photo}{}^{b}$	$k_{app} \times 10^{-3}$ (min^{-1})	$R^{2\,a}$	$A_{photo}{}^{b}$
TiO_2	6.8	5.02	0.9973	1.00	4.41	0.9980	1.00
$TiO_2- AC_{CO_2-800}$	14.8	6.83	0.9936	1.4	5.02	0.9866	1.2
$TiO_2- AC_{ZnCl_2-5\%}$	13.1	5.22	0.9878	1.1	3.45	0.9826	0.8
$TiO_2- AC_{N_2-1000}$	15.8	4.82	0.9894	1.0	3.16	0.9764	0.7
$TiO_2- AC_{H_3PO_4-5\%}$	10.3	5.53	0.9883	1.1	4.14	0.9782	0.9

[a]R is the square factor of the lineal regression. [b]Photocatalytic activity relative to TiO_2 defined as $\mathbf{A_{photo}} = \left(k_{app-i}/k_{app-TiO_2} \right)$.

our group has been previously reported for the case of the 4-chlorophenol photodegradation [5,7] that AC_{CO_2} has a more intimated interaction than AC_{N_2} with the Ti atoms in TiO_2. We have shown that this interaction occurs by means of a common contact interface [7] spontaneously created during reaction between both solids by the coordination the oxygenated functional groups on AC_{CO_2}, mainly cyclic ethers and carboxylate anions (**Figure 1**). This interaction is clearly lower for the case of TiO_2 and AC_{N_2} than with AC_{CO_2} because AC_{N_2} has lower oxygen surface composition than that of AC_{CO_2}, about 7% against 12 wt%, respectively [5].
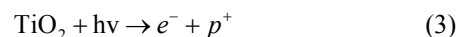
Figure 7 shows the kinetic of hydroquinone (HQ) and benzoquinone (BQ) appearance and disappearance during phenol photodegradation under UV-irradiated some selected solids. These two molecules were the main intermediates products observed in all samples studied and under both types of irradiation. The maximum time of appearance and time require for the total disappearance of intermediates are lower for the binary materials TiO_2-AC with respect to TiO_2 alone, only in presence of mixed system that showed higher photocatalytic activity. This fact is an indicative that intermediates products are also photodegradated in shorter irradiation time than that on TiO_2 reported by our group for the case of 4-chlorophenol [7,8]. As we appointed above, an explanation for the apparent synergy effect can be based on the conventional Langmuir-Hinshelnwood mechanism with the rate being proportional to the surface coverage θ varying as:

$$r = k\theta = k\left[K_{ads} \cdot C_{eq} \big/ \left(1 + K_{ads} \cdot C_{eq} + \Sigma K_i C_i \right) \right]. \quad (1)$$
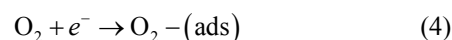
being: K_{ads} and K_i correspond to the adsorption constants of phenol and the intermediate i, C_{eq} and C_i is the phenol and intermediate concentration in solution after achieve the equilibrium adsorption in the dark. Owing to the similarity of the reactants and of the main initial aromatic intermediates formed, the term $\Sigma K_i \cdot C_i$ can be estimated as constant, thus explaining the apparent first order:

$$r \approx k\left[K_{ads} \cdot C_{eq} \big/ \left(1 + \Sigma K_i C_i \right) \right] = K_{ads} \cdot C_{eq} \quad (2)$$
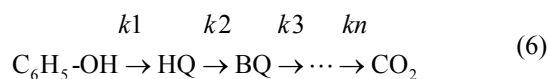
The nature of the intermediate main products (HQ and BQ) is the same for TiO_2-AC as for neat TiO_2. This confirms that reaction mechanism has not been altered nor changed by the addition of AC, or at least, for these carbons [15]. UV photons create electron hole pairs in Titania

$$TiO_2 + h\nu \rightarrow e^- + p^+ \quad (3)$$

which separate because of electron transfer reactions:

$$O_2 + e^- \rightarrow O_2 - (ads) \quad (4)$$

$$O_2 + p^+ \rightarrow OH^\circ. \quad (5)$$

As we have already appointed in previous works [15] OH° radicals created by Equation (5) react with phenolic compounds to produce hydroxylated aromatic compounds, mainly hydroquinone in equilibrium with benzoquinone (**Figure 7**), and then aliphatic fragments resulting from the opening before producing CO_2 such as picric acid, oxalic acids, and humic acids, are difficult to well quantified by HPLC. Thus, synergy effect can also be pointed out in the kinetics of intermediate products appearance and disappearance. For hydroquinone, its kinetics can be summarized as:

$$\begin{array}{ccccc} k1 & k2 & k3 & kn \\ C_6H_5\text{-}OH \rightarrow HQ \rightarrow BQ \rightarrow \cdots \rightarrow CO_2 \end{array} \quad (6)$$

4. Conclusions

For the case of MB photodegradation, the binary materials TiO_2-AC showed a clear increase in the photocatalytic activity with respect to TiO_2 alone, under the two lamps studied. Under the MH lamp which has a higher proportion of visible light, TiO_2 in presence of H-type AC showed higher photocatalytic activity with respect to TiO_2 in presence of L-type AC. This beneficial effect has been attributed to the specific properties of H-type AC with a high surface area and basic pH_{PZC}. By contrast, for the case of phenol photodegradation, only $TiO_2- AC_{CO_2-800}$
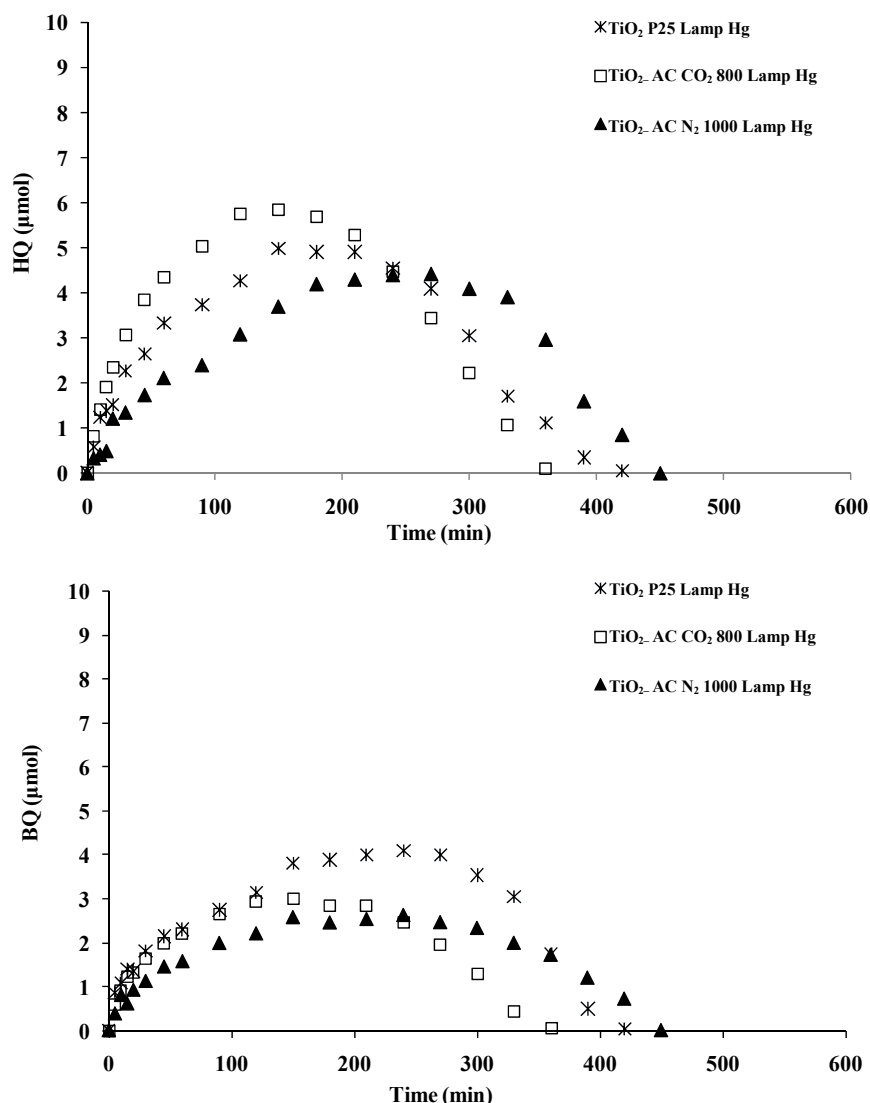
Figure 7. Hydroquinone (HQ) and benzoquinone (BQ) appearance and disappearance during phenol photodegradation with some selected solids under Hg Lamp.

presented higher photocatalytic activity than TiO_2.

REFERENCES

[1] A. Houas, H. Lachheb, M. Ksibi, E. Elaloui, C. Guillard and J. M. Herrmann, "Photocatalytic Degradation Pathway of Methylene Blue in Water," *Applied Catalysis B*: *Environmental*, Vol. 31, No. 2, 2001, pp. 145-157. doi:10.1016/S0926-3373(00)00276-9

[2] J. M. Herrmann, C. Guillard and P. Pichat, "Heterogeneous Photocatalysis: An Emerging Technology for Water Treatment," *Catalysis Today*, Vol. 17, No. 1-2, 1993, pp. 7-20. doi:10.1016/0920-5861(93)80003-J

[3] O. Legrini and E. Oliveros, "Photochemical Processes for Water Treatment," *Chemical Reviews*, Vol. 93, No. 2, 1993, pp. 671-698. doi:10.1021/cr00018a003

[4] J. M. Herrmann, J. Didier and P. Pichat, "Effect of Chromium Doping on the Electrical and Catalytic Properties of Powder Titania under UV and Visible Illumination," *Chemical Physics Letters*, Vol. 108, No. 6, 1984, pp. 618-622. doi:10.1016/0009-2614(84)85067-8

[5] T. Cordero, J. M. Chovelon, C. Duchamp, C. Ferronato and J. Matos, "Surface Nano-Aggregation and Photocatalytic Activity of TiO_2 on H-Type Activated Carbons," *Applied Catalysis B*: *Environmental*, Vol. 73, No. 3-4, 2007, pp. 227-235. doi:10.1016/j.apcatb.2006.10.012

[6] T. Cordero, C. Duchamp, J. M. Chovelon, C. Ferronato and J. Matos, "Influence of L-Type Activated Carbons on Photocatalytic Activity of TiO_2 in 4-Chlorophenol Photodegradation," *Journal of Photochemistry and Photobiology A*: *Chemistry*, Vol. 191, No. 2-3, 2007, pp. 122-131. doi:10.1016/j.jphotochem.2007.04.012

[7] J. Matos, A. García and P. S. Poon, "Environmental

Green Chemistry Applications of Nanoporous Carbons," *Journal of Materials Science*, Vol. 45, No. 18, 2010, pp. 4934-4944. doi:10.1007/s10853-009-4184-2

[8] J. Matos, A. García, T. Cordero, J. M. Chovelon and C. Ferronato, "Eco-Friendly TiO$_2$-AC Photocatalyst for the Selective Photooxidation of 4-Chlorophenol," *Catalysis Letter*, Vol. 130, No. 3-4, 2009, pp. 568-574. doi:10.1007/s10562-009-9989-8

[9] W. Wang, C. Gomes and J. L. Faria, "Photocatalytic Degradation of Chromotrope 2R Using Nanocrystalline TiO$_2$/Activated-Carbon Composite Catalysts," *Applied Catalysis B*: *Enviromental*, Vol. 70, No. 1-4, 2007, pp. 470-478.

[10] J. M. Peralta-Hernández, J. Manríquez, Y. Meas-Vong, F. J. Rodríguez, T. W. Chapman, M. I. Maldonado and L. A. Godínez, "Photocatalytic Properties of Nano-Structured TiO$_2$-Carbon Films Obtained by Means of Electrophoretic Deposition," *Journal of Hazardous Materials*, Vol. 147, No. 1-2, 2007, pp. 588-593. doi:10.1016/j.jhazmat.2007.01.053

[11] J. Matos, A. Garcia, L. Zhao and M. M. Titirici, "Solvothermal Carbon-Doped TiO$_2$ Photocatalyst for the Enhanced Methylene Blue Degradation under Visible Light," *Applied Catalysis A*: *General*, Vol. 390, No. 1-2, 2010, pp. 175-182. doi:10.1016/j.apcata.2010.10.009

[12] J. Matos, E. García-López, L. Palmisano, A. García and G. Marci, "Influence of Activated Carbon in TiO$_2$ and ZnO Mediated Photo-Assisted Degradation of 2-Propanol in Gas-Solid Regime," *Applied Catalysis B*: *Environmental*, Vol. 99, No. 1-2, 2010, pp. 170-180. doi:10.1016/j.apcatb.2010.06.014

[13] A. P. Terzyk, "The Influence of Activated Carbon Surface Chemical Composition on the Adsorption of Acetaminophen (Paracetamol) *in Vitro*: Part II. TG, FTIR, and XPS Analysis of Carbons and the Temperature Dependence of Adsorption Kinetics at the Neutral pH," *Colloids and Surfaces A*: *Physicochemical and Engineering Aspects*, Vol. 177, No. 1, 2001, pp. 23-45. doi:10.1016/S0927-7757(00)00594-X

[14] J. Matos, T. Marino, R. Molinari and H. García, "Hydrogen Photoproduction under Visible Irradiation of Au-TiO$_2$/Activated Carbon," *Applied Catalysis A*: *General*, Vol. 417-418, 2012, pp. 263-272. doi:10.1016/j.apcata.2011.12.047

[15] J. Matos, J. Laine, J. M. Herrmann, D. Uzcategui and J. L. Brito, "Influence of Activated Carbon upon Titania on Aqueous Photocatalytic Consecutive Runs of Phenol Photodegradation," *Applied Catalysis B*: *Environmental*, Vol. 70, 2007, pp. 461-469. doi:10.1016/j.apcatb.2005.10.040